Effect of Coagulation Conditions on Properties of Poly(acrylonitrile–carboxylic acid) Fibers

S. H. Bahrami,[1] P. Bajaj,[2,†] K. Sen[2]

[1]*Textile Engineering Department, Amirkabir University of Technology, Tehran, Iran*
[2]*Textile Technology Department, I.I.T., New Delhi, India*

Received 8 May 2001; accepted 24 October 2002

ABSTRACT: Acrylic fibers are among the most useful synthetic fibers for textile applications, and special acrylic fiber (SAF) has industrial applications. The physical and mechanical properties of fiber are affected by several parameters; one such parameter is coagulation conditions: bath temperature, bath composition, and drawing. Acrylonitrile–carboxylic acid copolymers, that is, acrylic methacrylic and itaconic acid, were converted into fibers using the dry-jet wet spinning technique. The coagulation bath temperature was varied from 5°C to 35°C, and the properties of the fibers so obtained were investigated. The effect of the final drawing ratios (6.5 and 8.5) on such physical and mechanical properties as tenacity, sonic modulus, initial modulus, density, crystallinity index, and X-ray orientation were also investigated. In addition, thermogravimetric analysis and scanning electron microscopy were used to determine the thermomechanical properties and fracture morphology of the fibers. © 2003 Wiley Periodicals, Inc. J Appl Polym Sci 89: 1825–1837, 2003

INTRODUCTION

Acrylic fibers spun from polyacrylonitrile homopolymer suffer from poor hygroscopicity and low dye pickup because of a high degree of ordering, a lack of segmental mobility as a result of a compact structure, and a high glass-transition temperature (T_g). Acrylic fibers therefore are essentially copolymers of acrylonitrile containing one or more comonomers that substantially improve the processibility as well as the dyeability of the fiber. Comonomers used in the manufacturing of acrylic fibers can be either neutral or ionic.

Neutral comonomers, such as methyl acrylate, methyl methacrylate, and vinyl acetate, modify the structure of polyacrylonitrile; the resulting reduction in compactness of the fibers increases the diffusion of the dyes. Polar, nonionizable comonomers, such as ketones, ethers, and alcohols, increase dye adsorption by enhancing nonionic interactions with the dyes.[1–4]

On the other hand, the use of ionic acidic comonomers containing sulfonic, phosphoric, or carboxylic acid groups influences both the rate of diffusion and the uptake of cationic dyes. The use of basic comonomers, such as 2-vinyl pyridine imparts the fiber with substantiality for anionic dyes; differentially dyeable fiber variants provide interesting commercial possibilities.

Commercially available acrylic fibers comprise 6%–7% by weight of neutral comonomers like vinyl acetate or methyl acrylate; this increase the solubility of the polymer in the spinning solution, modifies the morphology of the fibers, and reduces the glass-transition temperature (T_g), thereby improving the diffusion of dyes. In addition, 0.5%–1.0% ionic comonomers, such as sodium methallyl sulfonate, sodium styrene sulfonate, sodium sulfophenyl methallyl ether, and sodium salt of 2-acrylamido-2-methyl propane sulfonic acid (SAMPS), are used to supplement cationic dye sites.[3,5]

Hydrophilic fibers

Hydrophilicity of acrylic fibers can be enhanced by the incorporation of hydrophilic moieties as comonomers during polymerization or as dope additives before spinning the fibers. Many attempts have been made to produce hydrophilic acrylic fibers by copolymerization of acrylonitrile with vinyl monomers containing functional groups such as hydroxyl, ester, carboxyl, amide, and substituted amides. Hydrophilic acrylic fibers with good dyeability have been produced from copolymers of acrylonitrile containing 1.0–4.8 mol % of 2-hydroxypropyl methacrylate and 2-hydroxyethyl methacrylate as comonomers.[6] Fibers from acrylonitrile- *N,N*-dimethyl acrylamide copolymers have been shown to have hydrophilicity and acid dyeable properties. Terpolymers of acrylonitrile-methyacrylate and carboxylic acids, such as acrylic, methacrylic and itac-

Correspondence to: S. H. Bahrami (hajirb@aut.ac.ir).
†Dr. P. Bajaj passed away on 23 May 2002.

Journal of Applied Polymer Science, Vol. 89, 1825–1837 (2003)

onic acids, have shown good dye sorption.[7] Acrylonitrile (AN) terpolymers containing 4%–9% methacrylate (MA) and 1.5%–6% acrylic or methacrylic acid was solution-spun using 10%–12% sodium thiocyanate as the coagulant.

The hygroscopicity and dyeability of acrylic fibers have been improved by blending fibroin[8] and collagen (5%–15%),[9] polycapromide, chitin, polyvinyl acetate, and hydrolyzed acrylonitrile copolymer.[10,11]

Bajaj and Surya[12] also studied the dyeing behavior of acrylic fibers containing hydrolyzed acrylonitrile terpolymer, secondary cellulose acetate, polyvinyl pyrrolidone, glycerol, and polyvinyl acetate as dope additives. These blended fibers have higher diffusion coefficients and require a lower activation energy of dyeing.

Bajaj[13] reported the development of a new hydrophilic acrylic fiber that has 25%–35% water absorption. It is suitable for the climatic conditions prevailing in tropical countries. This microporous acrylic fiber has been produced by conjugate spinning of poly(AN–MA–SAMPS) with a cellulose derivative. According to Bajaj, high water-retentive acrylic fiber was developed by blending conventional acrylonitrile terpolymers—that is, acrylonitrile, methyacrylate, and sodium methyl propenyl sulfonate (90.9:8.6:0.5 wt %) with a molecular weight of 72,000—with a small amount of polyvinyl acetate, polystyrene, or acrylonitrile—vinyl acetate copolymers.[14] He demonstrated that incompatibility and phase separation are important requisites for producing high water-retentive microporous acrylic fibers. The criterion for incompatibility is the difference in the solubility parameter of the constituents of the blend used for producing microporous acrylic fibers.

Effect of spinning conditions on structure and morphology of acrylic fibers

Spinning solutions (dope) with polymer concentrations ranging from 10% to 25% are generally used for the production of acrylic fibers by the wet-spinning process.[15] The solid content in the dope depends on the molecular weight and the nature of the solvent. With an increase in the concentration of the polymer (at a constant molecular weight) in the dope, the spinnability can be improved,[16] the tenacity increased,[17] and the porosity reduced in the cross section of the fibers.[18,19]

Knudsen[20] observed that increasing the dope solids (15%–25%) improves the homogeneity of the fiber structure by reducing the generation of large voids, increases the density, and slightly improves the tenacity. The effect of the dope concentration of poly(AN–MMA) copolymer on the structural and mechanical properties of acrylic fibers has also been investigated by Stoyanov.[15] The influence of the polymer concentration on the various diffusion processes taking place in the coagulating bath was explained as based on fiber breakage mechanisms, as proposed by Paul,[32] and Han and Segal.[21] Takahashi et al.[22] studied the effect of fiber-forming conditions on the microstructure of acrylic fibers. When the coagulation bath consisted only of water as the nonsolvent, the cross section of fiber showed many voids. However, as the concentration of dimethylsulfoxide solvent increased in spinning bath, the number of voids also decreased; at 70% DMSO the protofibers showed no voids. The content of microvoids in the filaments obtained by spinning into aqueous baths in many cases was markedly larger than that in the filaments obtained by spinning into the nonaqueous baths. The bath temperature also affected the microvoids. The lower the bath temperature, the fewer were the number of voids. The effect of coagulation bath composition and temperature on the structure of protofibers was reported by Knudsen.[20] In this study the spin bath concentration of dimethyl acetamide was kept constant at 55%, whereas the coagulation bath temperature was varied from 0°C to 70°C. A progressive improvement in fiber density, an increase in internal surface, and a reduction in the number of large voids were observed with decreasing spin bath temperature.

In wet spinning microscopic and morphological structures as well as mechanical properties are strongly influenced by the mass transfer between the spinning line and the surrounding medium, that is, the coagulation bath. The cross section of wet-spun fibers becomes more circular at a higher bath temperature,[20,23] with a higher solid content in the dope,[24] and with a higher solvent content in the coagulation bath.[25]

Tsai and Su[19] found in their study, in which a Y-shaped spinneret was used, that it was possible to produce Y-shaped homogeneous acrylic fibers at a higher coagulation temperature, which is also a key variable controlling the diffusion of solvent and nonsolvent as well as the cross-sectional shape of the acrylic fibers. As in most diffusion processes, an elevation in temperature, either of the dope or the coagulation bath, increases the diffusion of solvent and nonsolvent. However, the diffusion rate for the solvent increases faster than that for the nonsolvent.

In an interesting study Pakshver et al.[26] showed that by adding water to a spinning dope of poly(AN–IA) copolymer in dimethylformamide (DMF containing 2% itaconic acid by weight, IA accelerated the gelation process and increased the temperature for gelation. In spinning from such solutions, the process of fiber solidification takes place by two mechanisms: diffusion and cooling. It is assumed that the addition of water to the spinning solution shifts the solidification process in the direction of the cooling mechanism, leading to more uniform and better-oriented acrylic fibers.

Ergashev et al.[27] have also demonstrated the use of isopropyl alcohol in the spinning dope of the ternary polymer, poly(AN–MA–IA, in a ratio of 92:6.4:1.6 (wt %), and a copolymer of AN–MA in DMF. The addition of 6% isopropyl alcohol in the spinning solution decreased its viscosity and spinnability, consequently decreasing the elastic part of the fiber deformation. In this manner the physicomechanical properties of the fibers thus spun can be regulated. The tenacity of poly(AN–MA) copolymer fibers produced from a spinning dope containing 6% isopropyl alcohol was found to be 400 mN/tex, much higher than that produced from a neat dope without isopropyl alcohol (240 mN/tex). From the foregoing discussion it may be concluded that diffusion is the fundamental process governing the fiber structure produced during wet spinning. Given the main variables of a polymer-spinning solution (dope) and coagulation bath, many investigators[28–33] have derived mathematical models relating the time to coagulate an extruded filament and the diffusion rate of the solvent and nonsolvent and thus have estimated the diffusion coefficients for a variety of spinning systems. Paul,[32] using the gelation of large cylindrical rods, showed that the solvent diffusion was a function of the square root of the gelation time.

Recent investigations that used modeling techniques to understand diffusion processes have been reported by Baojun et al.,[30] Alieva et al.,[34] and Dolzhikov et al.[35] Baojun and coworkers[30] used a dimethylformamide–water system for a coagulation bath. Diffusion coefficients and flux ratio as functions of jet stretch, polymer solution concentration, and coagulation temperature have been calculated. Diffusion coefficients were found to be in the same range, 4–10 $\times 10^{-6}$ cm^2/s, as that found by Paul for the DMAc–H_2O system. Diffusion models, however, do not predict fiber structure. It is likely that incorporation of the contribution of the phase-separation phenomenon into the diffusion models would make these more relevant for the prediction of fiber properties.

An interesting variation of wet spinning is known as dry-jet wet spinning, or air-gap spinning.[6,36] In this process the spinneret is located a short distance (< 10 mm) above the spin bath, with the filaments extruding vertically into the fluid. The advantage of this method is having the ability to control the dope temperature independent of the spin-bath temperature. This technique also avoids high stress on the protofilaments at the jet face, which occurs in wet spinning. Dry-jet wet spinning therefore is recommended for producing high-strength acrylic filaments.

Effect of drawing conditions on structure properties of acrylic fibers

The stretching process is very important in altering fiber structure and enhancing fiber properties. Normally, stretching is done above the wet T_g (for instance, in hot water), and the fiber is stretched 3–12 times. In this stretching process the orientation of the fibrillar network (formed in the spin bath) increases, thereby improving the fiber strength.

In one study a series of wet-spun poly (acrylonitrile–vinyl acetate) fibers were hot-wet-stretched to a draw ratio of 2×–7× for studying their surface morphology and frictional characteristics. These drawn fibers showed an increase in molecular orientation and structural compactness. The fiber-to-fiber coefficient of friction also increased with draw ratio, providing an excellent correlation between orientation and friction.[37] Thermal drawing of poly(AN–IA) copolymer fibers after plasticization drawing has also been suggested as a way to obtain high-strength fibers. The plasticization drawing (λ) was varied from 3.0 to 7.0.[38] The samples were subsequently thermally drawn in an air tube 0.75 m long to the maximum possible ratio with a step of $\Delta\lambda_{therm} = 1.3$. An increase in the plasticization drawing ratio from $\lambda = 3$ to $\lambda = 7$ was accompanied by an increase in the strength of the samples from 0.35 to 0.53 GPa and of the initial modulus from 9.5 to 11.2 GPa, with a consequent decrease in elongation at break from 14% to 12%.

The effect of molecular weight, molecular weight distribution, and degree of stretch on the physicomechanical properties of the acrylic fibers have been well documented. The terpolymers (AM:MA:AA 93:4:3 wt %) having an intrinsic viscosity [η] of 2.6–2.8 with a narrow molecular weight distribution and 900% plasticized stretch produced fibers having a tenacity of 72 cN/tex.[7] However, the fibers spun from a 12% solution of AN–MA–IA terpolymer with an intrinsic viscosity [η] of 1.9 had a tenacity of 31.2 cN/tex and an elongation at break of 23.2% when stretched to 700%. Law and Mukhopadayay have studied the acrylic fiber formation by the wet-spinning technique using NaSCN as solvent.[39] They also studied the compositional changes taking place during the wet spinning.[40–43]

In this article the results of solution spinning of acrylonitrile–carboxylic acid copolymers—acrylonitrile–acrylic acid copolymer (PA), acrylonitrile–methacrylic acid copolymer (PM), and acrylonitrile–itaconic acid copolymer (PI)—using dry-jet wet-spinning technique are reported. The effect of coagulation bath temperature and stretching conditions on the structure properties of acrylic fibers spun therefrom have also been investigated.

EXPERIMENTAL

Materials

Three copolymers of acrylonitrile–carboxylic acid—acrylic (AA), methacrylic (MAA), and itaconic (IA)—

TABLE I
Ball Fall Data for Acrylonitrile–Carboxylic Acid Copolymers

Copolymer and [η]	Dope solids (wt %)	Ball fall time (s) at different temperatures (°C)						
		30	40	50	60	70	80	90
Poly(AN–AA) [η] = 1.30	20	98.3	67.4	47.9	38.2	29.3	27.9	26.1
Poly(AN–MAA) [η] = 1.35	18	116	73.2	50.8	40	31.9	25.2	24.3
Poly(AN–IA) [η] = 1.24	23	104.3	70.2	51.8	35.8	30.8	26.6	25

with 2.2–3.1 mol % of acid in the copolymer of [η] = 1.24–1.35 were selected for spinning. The method of synthesizing these copolymers was reported elsewhere.[44] On the basis of ball fall viscosity data, dopes of different solid contents but nearly the same ball fall time at 60°C were made by stripping off the unreacted monomers and removing the extra solvent by vacuum extraction. The dope was used directly for spinning. Characteristics of the acrylic copolymers and the viscosity of the dope are given in Table I.

Dry-jet wet spinning

The copolymers were spun using the dry-jet wet-spinning technique on a laboratory solution spinning line. The dope was passed through a spinneret of 100 holes. The temperature of the coagulation bath was varied from 5°C to 35°C. The protofibers were first collected at this point for structural investigation and then passed over the roller into the second bath, which contained DMF:H_2O.

Plasticized fibers were stretched up to a 1.65 draw ratio at this stage. The fibers were then washed in a bath containing dimineralized water and were further stretched, up to a 1.8 draw ratio, at 70°C. The fibers were subsequently washed in DM water at boil and drawn up to 2 DR. A 1% spin finish (APAN 41 + 43D) was applied onto the fibers and then was passed over a heater plate at 140°C. The total draw ratio including relaxation applied on the fiber was 6.5. Fibers collected at this stage are referred to as first zone–drawn samples. Additional drawing of the fibers was carried out on a second heater plate at 160°C so as to get a total draw ratio of 8.5. The fibers collected at this stage are referred to as second-zone-drawn fibers. The spinning and drawing conditions are given in Table II.

Evaluation of gel fibers

It is essential to study the uncollapsed fiber structure as it exits from the coagulation bath in order to understand the actual influence of coagulation bath variables on fiber structure. To do this, samples were taken from the coagulation bath (gel- or protofibers), washed thoroughly with cold distilled water, and preserved at low temperature before studying such characteristics as shape, density, and mechanical properties.

The shape of the gel fibers, collected at different coagulation bath temperatures, was studied under an optical microscope using 500× magnification after cutting them into cross sections. The spinning conditions along with the fiber codes are listed in Table III.

Evaluation of structure properties

Density measurement was carried out using a density gradient column (Daven Port, London) comprising a mixture of *n*-heptane and carbon tetrachloride at 25°C.

Wide-angle X-ray diffraction patterns were recorded using nickel-filtered CuK radiation. The generator (Philips Electronic Instruments) was operated at 30 KV voltage and 30 mA current for acquiring the average size of the laterally ordered phase (crystal size) and the extent of order. Finely chopped fibers were pressed into a flat plate, and equatorial intensity scans in the range of 2θ = 5°–35° were obtained. The size of the ordered domains was estimated by the Scherrer equation:

$$L_c = \frac{K^{\lambda}}{\beta \cos \theta}$$

TABLE II
Dry-Jet Wet—Spinning Conditions

Copolymer	PA, PM, PI
Spinning	
Number of holes	100
Diameter	0.1 mm/hole
Dope temperature	60°C
Throughput rate	0.98 g/min/100/hole
Coagulations	
Bath I	DMF:H_2O (60:40 v/v)
Bath II	Dmf:H_2O (10:90 v/v) λ_2 = 1.65
Washing	
Bath III	DM water 70°C λ_2 = 1.8
Bath IV	Boiling water λ_3 = 2
Spin finish	APAN 41 + 43 D (1%)
Stretching	
Zone I	First heater plate λ_4 = 1.1
Zone II	Temperature 140°C λ_{total} = 6.5
	Second Heater
	Temperature 160°C λ_{total} = 8.5

TABLE III
Spinning Conditions and Codes of the Fibers

Copolymer composition (mol %)	First bath DMF:H_2O Temperature (°C)	Second bath DMF:H_2O Temp. °C	Washing bath DM water		Drawing		Fiber code	
			Third bath Temperature (°C)	Fourth bath Temperature (°C)	First zone 140°C	Second zone 160°C	First zone	Second zone
Poly(AN–AA) AA = 3.1%	5	40	70	Boiling water	DR = 6.5	DR = 8.5	FA 5	FA5D
	15						FA 15	FA15D
	25						FA 25	FA25D
	35						FA 35	FA35D
Poly(AN–MAA) MAA = 2.6%	5	40	70	Boiling water	DR = 6.5	DR = 8.5	FM 5	FM5D
	15						FM 15	FM15D
	25						FM 25	FM25D
	35						FM 35	FM35D
Poly(AN–IA) IA = 2.2%	5	40	70	Boiling water	DR = 6.5	DR = 8.5	FI 5	FI5D
	15						FI 15	FI15D
	25						FI 25	FI25D
	35						FI 35	FI35D

where L_c is the average lateral size (crystal size); β is the full width at half maximum intensity at $2\theta = 17°$; K is the Scherrer constant (0.89); and λ is the wavelength of the X-ray used (1.54 A).

Corrections for nonhomogeneous strains and instrumental broadening were neglected in these calculations. The extent of order was calculated from the intensity plot by the method suggested by Gupta and Singhal, assuming reflections at $\theta = 17°$ to be a result of the crystalline region.

To obtain the orientation index of the lateral order phase, fiber bundles were wound carefully on the sample holder to parallelize them. Orientation was determined from the azimuthal scan at $2\theta = 17°$. The width at half maximum intensity ($H = I_{1/2}$) was used as an index of orientation, which may be used to calculate the parallelism of the crystalline part of structure by the following equation.[45]

$$P = \frac{90 - H/2}{90} \times 100\%$$

In addition, to investigate the crystallite orientation, a bundle of parallel filaments was also wound on a specimen holder of a flat plate camera (mounted perpendicular to the path of the X-ray beam) and exposed for 4 h with a film distance of 3.5 cm, after which the film was processed under standard conditions.

Sonic modulus

The sonic modulus of the fibers was measured on a pulse propagation meter (PPM-5), H. M. Morgan Sonic modulus tester (USA). The velocity of sonic pulse through the filament in kilometers per second, that is, sonic velocity (C) was calculated as:

$$C = \frac{\text{Scanning distance in millimeters}}{\text{Transit time of pulse in microsecond}}$$

where K is 11.3 (constant conversion factor); C is the sound velocity (km/s); and E (g/d) is $C^2 \times 11.3$.

The mechanical properties of the single filaments were tested on an Instron Tensile Tester model 4301 at the standard ambient conditions, that is, RH = 65% ± 2% and temperature of 25°C ± 2°C. The method suggested by Urquhart and Williams was used for determining the moisture regain. The difference between the weight of the sample keptat 65% RH and 25°C for 2 days (w_2) and that of the sample kept over P_2O_5 until a constant weight (w_1) was used for calculating the moisture regained as follows:

$$\text{Moisture regain} = \left(\frac{w_2 - w_1}{w_1}\right) \times 100$$

Boiling water shrinkage was measured by freely suspending the known length of the filament yarn under a 0.1 gpd load in the boiling water for 5 min. The change in length was used to calculate the shrinkage using the following expression:

$$\%S = \frac{L_o - L_s}{L_o} \times 100$$

where L_o is the initial length and L_s is the length after shrinkage.

A glass cylinder 30 cm in height and 2 cm in diameter (with one end closed) and stainless-steel balls each weighing 0.127 g were used for this test. Polymer dope of different solid contents was taken in this cylinder and kept in a water bath maintained at a specified temperature. A ball was placed on the sur-

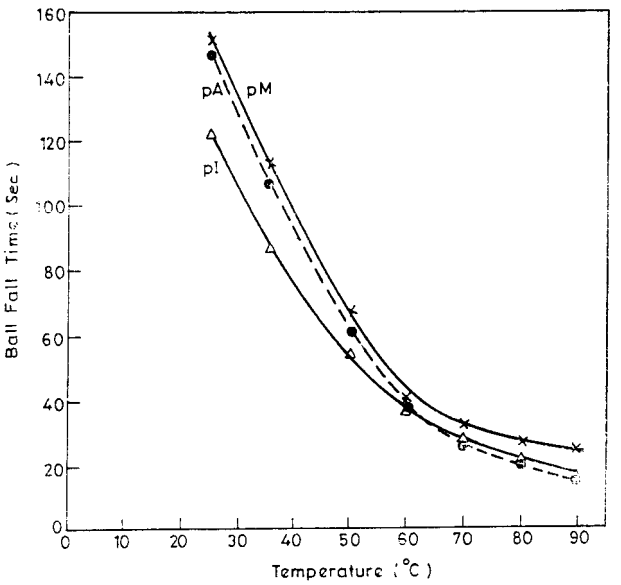

Figure 1 Dependence of ball-fall time on temperature of the spinning of dope, PI, PM, and PA.

face of the dope, and the time taken to travel between the marked points (20.8 cm) was noted at different temperatures. The fracture morphology of the acrylic fibers broken in the tensile test was characterized by a scanning electron microscope (Cambridge Stereoscan S 4-10). The samples mounted along with the cello tape were gold-coated before scanning.

RESULTS AND DISCUSSION

Dope viscosity

The solution spinning stage is primarily characterized by various flow processes and therefore is influenced to a large extent by the rheological properties of the dope. Copolymer solutions in DMF with varying solid contents (15%–25%) were prepared. Then 1% oxalic acid was added before measuring the viscosity at temperatures in the range of 30°C–90°C (Fig. 1). It is evident that the viscosity dropped considerably with an increase in the dope temperature from 30°C to 90°C for all the spinning dopes. This could be a result of the favorable flow orientation of the polymer chains and the disruption of the solvent-enveloped polymer at high temperatures, mainly because of increased kinetic energy.

The viscosity of concentrated polymer solutions depends largely on the association characteristics of the solvated acrylic copolymer macromolecules in dimethyl formamide. At 30°C the difference in ball fall time for three copolymers was in the range of 98.3–116 s, but with an increase in the dope temperature to 90°C, this reduced to 24.3–26.1 s. Because PA, PM, and PI had different intrinsic viscosity values, the solid contents were varied so as to get nearly the same ball fall time of the spinning dope at 60°C. In this manner it was possible to fix the throughput rate for extrusion of all the copolymers.

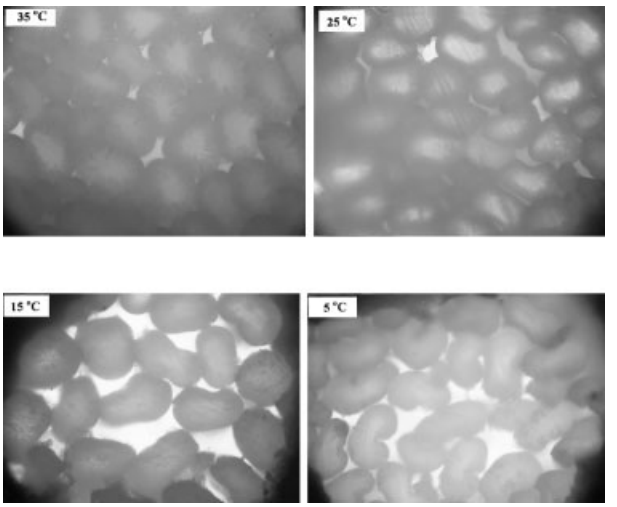

Figure 2 Effect of coagulation temperature on the shape of the gel fibers.

Effect of coagulation bath temperature

Gel fibers

The cross sections of the freeze-dried gel fibers collected after the first coagulation bath observed under an optical microscope are shown in Figure 2. As the coagulation bath temperature increased from 5°C to 35°C, there was a clear trend toward a more circular cross section of these fibers. The fibers that coagulated at 5°C attained a dumbbell-shaped cross section. Knudsen[20] reported that at a higher bath temperature, counterdiffusion of solvent and nonsolvent took place in approximately equal volumes across the fiber surface. As the coagulation temperature was reduced, the outward diffusion of solvent predominated, resulting

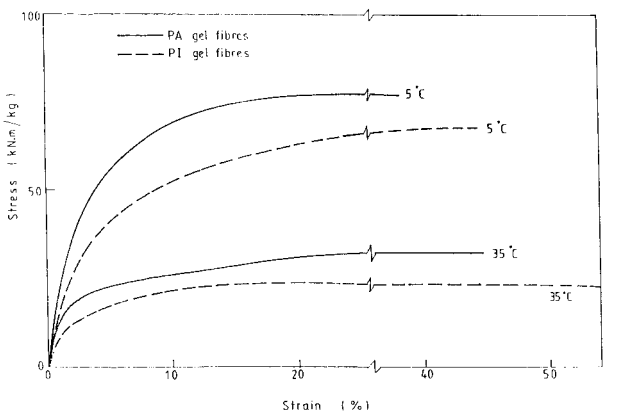

Figure 3 Stress–strain curves of gel spun fibers, PI, and PA coagulated at 5°C and 35°C.

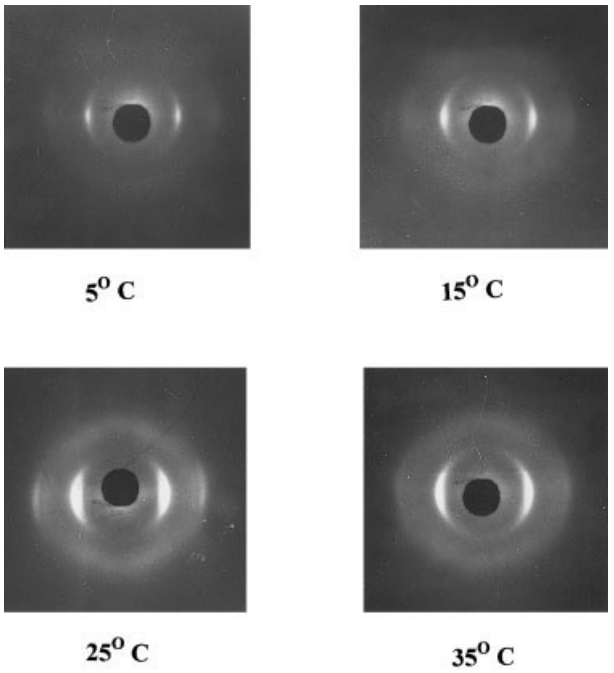

Figure 4 X-ray photograph of acrylic fiber (FM) produced at different coagulation bath temperatures and drawn to a total draw ratio 8.5.

in noncircular cross sections and gel fibers with small pore size and higher density.

The stress–strain behavior of the gel fibers is shown in Figure 3. The fibers showed poor tenacity and high elongation with possibly considerable drawing. The stress–strain curves had two distinct regions: one representing recoverable elastic, the other nonrecoverable plastic. The Hookean region of the curve may, be divided further, into two portions: the initial high modulus portion, which may be attributed to elastic glassy deformation (below T_g); and the recoverable strain portion, which results from the stretching of the helics of the PAN molecules. In the entire Hookean region the intermolecular bonds are stretched to their limit, and afterward, they or even the covalent bonds of the polymer chain may be ruptured. The stress–strain curves after the Hookean region could be assigned to irrecoverable flow, which causes an increase in the length and decrease in the entropy of the fibers.

The coagulation bath temperature affected the stress–strain behavior of the gel fibers. With a low temperature (5°C) in the coagulation bath, the PA gel fiber spun from poly(AN–AA) copolymer showed higher strength and modulus, whereas at 35°C the strength of the fiber was reduced and the elongation increased (Fig. 3).

Comparing the mechanical properties of gel fibers from different AN–carboxylic acid comonomers at 5°C showed that PM exhibited the greatest strength modulus, followed by PA and PI.

Gel fiber	Tenacity (kN m kg^{-1})	Elongation (%)
PA	78	39
PM	89	36
PI	70	44

Structure properties of acrylic fibers after first-zone drawing

The physical properties of the acrylic fibers were determined in large measure by the structure of the protofibers as these emerged from the coagulation bath, stretching washing baths, and drawing. And structure, in turn, was determined by the interplay of coagulation and drawing variables. The fibers were thus collected after first-zone drawing at 140°C with a draw ratio of 6.5 and evaluated.

Density

The density of these fibers varied between 1.165 and 1.180 g/cm^3. It can be seen from Table IV that the density decreased as the coagulation bath temperature

TABLE IV
Physical Properties of Fibers Collected after First-Zone of Drawing (DR = 6.5)

Fiber code	Den/fil	Density (g/cm^{-3})	X-ray crystallinity index	X-ray orientation (f %)	Crystal size (Lc)	Moisture regain (%)	Boiling water shrinkage (%)
FA 5	3.6	1.180	0.53	76	37	1.4	8.1
FM 5	3.6	1.177	0.56	79	42	1.3	7.2
F 15	3.4	1.176	0.53	72	35	4.3	9.4
FA 15	3.7	1.176	0.51	73	33	1.6	9.2
FM 15	3.8	1.173	0.55	78	37	1.4	8.4
FI 15	3.8	1.172	0.48	71	30	1.7	11.1
FA 25	3.6	1.173	0.48	73	27	1.6	10.1
FM 25	3.7	1.169	0.52	74	31	1.4	8.9
FI 25	4.1	1.169	0.47	65	24	1.8	11.0
FA 35	4.2	1.168	0.47	65	17	1.7	11.0
FM 35	4.1	1.165	0.50	67	20	1.5	9.8
FI 35	4.0	1.165	0.45	64	16	1.9	11.6

increased from 5°C to 35°C. In FA5 fiber density was 1.176 g/cm^3, whereas for the same copolymer, the fiber coagulated at 35°C (FA35), and the density was 1.165 g/cm^3.

This is because at low temperature the outward diffusion of the solvent predominates and there is more scope for internal adjustment of osmotic stresses, resulting in high-density fibers. However, a high coagulation temperature results in a fiber with higher skin content and higher porosity, thereby reducing the density. Comparing the three AN–carboxylic acid polymer fibers, the density of the PA fibers was highest, followed by PM, at a constant coagulating bath temperature. The strong dipole–dipole attraction between the nitrile groups of the adjacent chains was responsible for molecular packing in PAN. This attraction was progressively reduced because of incorporation of the AA, MAA, and IA pendant groups. Because IA is bulkier than AA and MAA, it is likely to reduce the molecular packing in a copolymer.

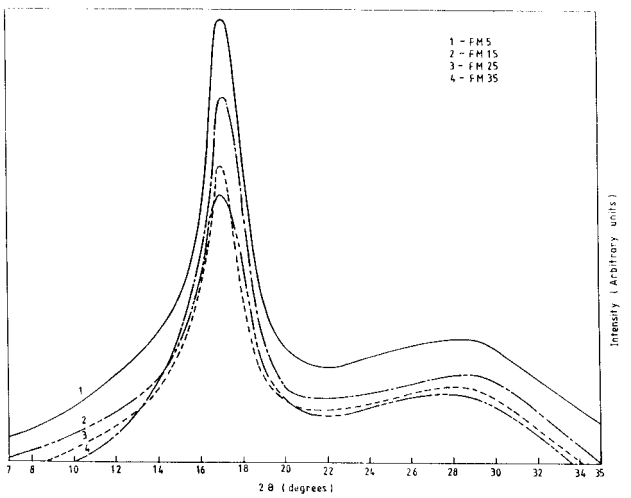

Figure 5 X-ray diffraction pattern of acrylic fiber (FM) produced at different coagulation bath temperatures and drawn up to an 8.5 draw ratio.

WAXD

Wide-angle X-ray diffraction (WAXD) photographs of parallelized fibers revealed two equatorial diffractions, one very intense, the other diffused. Such diffraction can be ascribed to the 110 and 020 planes, which have 0.52 and 0.33 nm repeat distances, respectively. The high intensity of the 110 diffraction is known to be associated with the preferential positioning of the nitrile group. As the coagulation bath temperature increased, two equatorial reflections became broad and more diffused (Fig. 4). This indicates a reduction in crystallinity and crystal size. A careful glance also reveals broadening of the arcs in the equatorial direction as the coagulation temperature was increased. This is indicative of a reduction in the crystallite orientation.

To investigate further, WAXD photographs of powdered samples were also studied. The X-ray diffraction patterns of the acrylonitrile–carboxylic acid copolymers showed an intense peak at $2\theta \sim 17°$ because of the main equatorial reflection from the 110 plane along with a diffused peak at $2\theta \sim 29°$ (Fig. 5).

As the coagulation bath temperature increased, a decrease in the intensity of the 110 peak with a concomitant broadening was observed. The decreased intensity indicates a possible reduction in the crystallinity, whereas the broadening represents a reduction in crystal size. Thus, rapid coagulation at higher temperatures is not conducive to crystal growth. For instance, FA5 fibers showed a crystallinity index of 0.53 and an average crystal size of 37 Å, whereas for FA35 these values reduced to 0.47 and 17 Å, respectively (Table IV).

Similarly, the crystalline orientation index also reduced from 76% to 65% for FA fibers produced at coagulation bath temperatures of 5°C and 35°C, respectively.

Mechanical properties

The effect of coagulation bath temperature on the mechanical properties of fibers is quite evident in all these cases. For instance, the tenacity of FM5 fibers spun at a 5°C coagulation bath temperature was 409 kN m kg^{-1}; however, as the coagulation bath temperature increased to 35°C, the tenacity dropped to 296 kN m kg^{-1} (Table V).

The presence of microvoids in the fibers spun at a higher coagulation bath temperature and low crystallinity and orientation may be responsible for the drop in strength of the fibers. The breaking elongation of the fibers spun at a low coagulation bath temperature was lower than that of fibers coagulated at a higher temperature. As the coagulation bath temperature increased, the elongation increased, too. The elongation at break of FI5 was 25.3, increasing to 35.1 for the FI35 fibers. The higher number of voids at higher temperatures may be responsible for this.

The initial modulus of fibers spun at a lower coagulation bath temperature was also higher (Table V). It gradually decreased as the coagulation bath temperature increased. For example, the initial modulus of FA5 was 8142 kN m kg^{-1}, whereas that of FA35 was 7077 kN m kg^{-1}.

The boiling water shrinkage of the fibers varied from 7.2% to 11.6% (Table IV). The temperature of the coagulation bath also played a significant role. The boiling water shrinkage of FI5 fibers was 9.4%, whereas that of fibers produced at a higher coagulation bath temperature (FI35) was 11.6%. Shrinkage is the response of the amorphous phase of the structure.

TABLE V
Mechanical Properties of Fibers Collected after First-Zone of Drawing (DR = 6.5)

Fiber code	Density (g/cm^{-3})	Tenacity [kN m kg^{-1} (cv %)]	Breaking elongation (%) (cv %)	Initial modulus [kN m kg^{-1} (cv %)]	Sonic modulus (kN m kg^{-1})
FA5	1.180	389 (14)	26.4 (20)	8142 (12)	13,717
FM5	1.177	409 (16)	23.7 (17)	8142 (10)	14,336
FI5	1.176	366 (13)	25.3 (16)	7522 (11)	13,009
FA15	1.176	347 (10)	29.2 (18)	7522 (13)	12,035
FM15	1.175	370 (9)	28.1 (21)	7788 (12)	13,388
FI15	1.173	328 (13)	26.3 (17)	7345 (11)	11,858
FA25	1.173	328 (11)	31.6 (16)	7345 (13)	12,035
FM25	1.171	356 (14)	30.3 (21)	7522 (15)	12,478
FI25	1.169	299 (13)	31.8 (19)	7080 (12)	12,635
FA35	1.168	298 (13)	35.5 (22)	7077 (13)	11,150
FM35	1.165	296 (14)	33.1 (23)	7180 (10)	11,416
FI35	1.165	260 (13)	35.1 (20)	6196 (11)	10,800

During spinning as the coagulation bath temperature increases, the crystallinity decreases, indicating a greater amorphous region.

Moisture regain

As the coagulation bath temperature was increased from 5°C to 35°C, the moisture regain of acrylonitrile–carboxylic acid fibers also increased (Table IV). Comonomers containing hydrophilic groups such as —OH and —COOH, have been reported to have enhanced moisture regain. The high moisture regain of fibers spun at higher coagulation bath temperatures may also be related to the high amorphous content of these fibers, which is evident from the X-ray crystallinity values and from the porosity. The highest moisture regain was obtained for fibers spun at 35°C. Among these, the fibers made from PI copolymer exhibited the most moisture regain. FI15 showed 1.7% moisture regain, whereas for FM15 and FA15 it was 1.4% and 1.6%, respectively.

Effect of second-zone drawing

Additional drawing affected the X-ray crystallinity marginally. For example, the crystallinity index of FM5 was 0.56 after the first-zone drawing, which increased to 0.59 after the second-zone drawing (Table VI). The X-ray orientation also was affected by drawing. For FM5 the orientation was 79, which increased to 81 for the fiber drawn, up to an 8.5 draw ratio (FM5D). A similar observation was made by Tsai and Su.[19]

Fiber density increased on drawing. The density of fibers spun from poly(AN–MAA) at 5°C and drawn up to DR = 6.5 (FM5) was 1.177 g/cm^3, which, on further drawing, up to TDR 8.5 (FM5D), increased to 1.180 g/cm^3. This is because as the fibers were drawn, the microvoids present on the fiber collapsed, and a more compact structure was formed.

Drawing of the fibers orients the molecular chains, resulting in improvement of the mechanical properties. Stress–strain curves of different AN–car-

TABLE VI
Physical Properties of Fibers Collected after Second Zone of Drawing (DR = 8.5)

Fiber code	Den/fil	Density (g/cm^{-3})	X-ray crystallinity index	X-ray orientation [(f) %]	Crystal size (Lc)	Moisture regain (%)	Boiling water shrinkage (%)
FA5D	3.2	1.182	0.55	79	39	1.3	7.8
FM5D	3.1	1.180	0.59	81	44	1.2	7.1
FI5D	3.0	1.178	0.54	76	37	1.3	9.2
FA15D	3.2	1.180	0.55	75	35	1.4	8.9
FM15D	3.3	1.176	0.58	81	40	1.3	8.0
FI15D	3.4	1.175	0.51	73	32	1.5	10.2
FA25D	3.3	1.175	0.52	74	29	1.5	9.8
FM25D	3.4	1.174	0.56	76	33	1.4	8.6
FI25D	3.8	1.172	0.50	68	25	1.7	10.8
FA35D	4.1	1.172	0.50	67	20	1.6	10.8
FM35D	4.1	1.169	0.54	69	21	1.4	9.1
FI35D	4.1	1.168	0.48	65	18	1.6	11.3

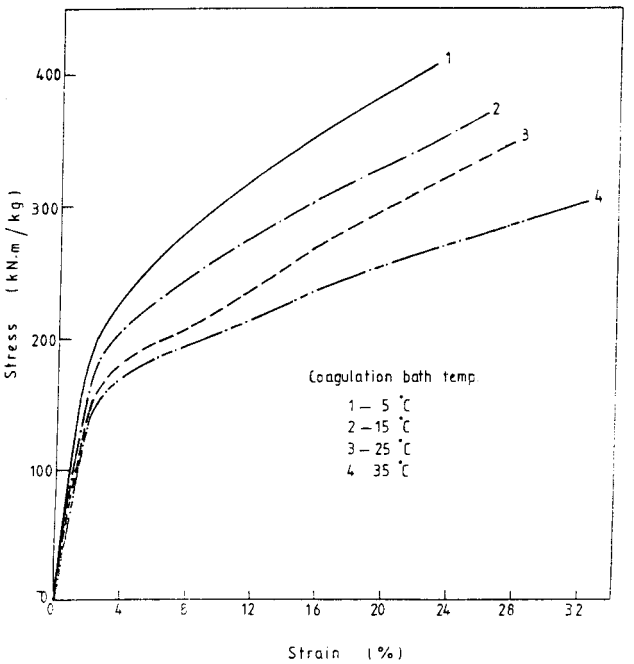

Figure 6 Stress–strain curves of FA fibers produced at different coagulation bath temperatures and drawn up to an 8.5 draw ratio.

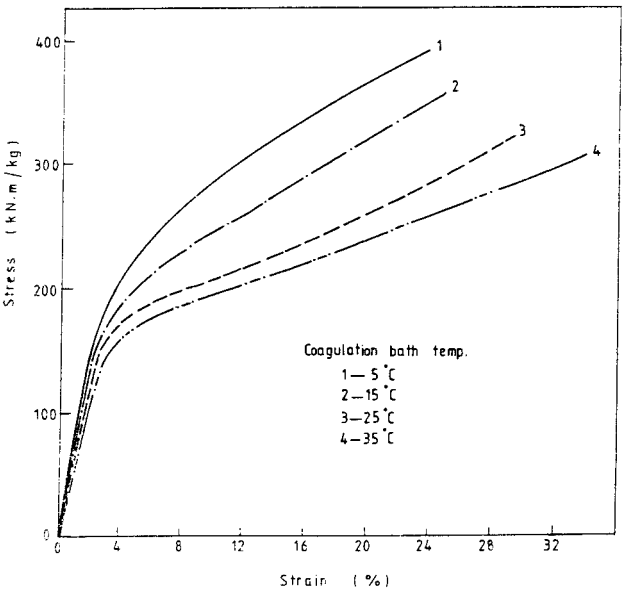

Figure 8 Stress–strain curves of FI fibers produced at different coagulation bath temperatures and drawn up to an 8.5 draw ratio.

boxylic acid copolymers spun at different coagulation bath temperatures is illustrated in Figures 6–8. The tenacity of FM15 spun at 15°C coagulation bath temperature and drawn up to a total draw ratio of 6.5 in the first drawing zone was 370 kN m kg^{-1}. However, when the same fibers were subjected to additional drawing in the second zone drawing up to TDR 8.5, that is, FM15D, the tenacity increased to 400 kN m kg^{-1}. The initial modulus also increased, from 7788 to 7965 kN m kg^{-1}. The elongation, on the other hand, decreased from 28.1% to 23.3% (Table VII).

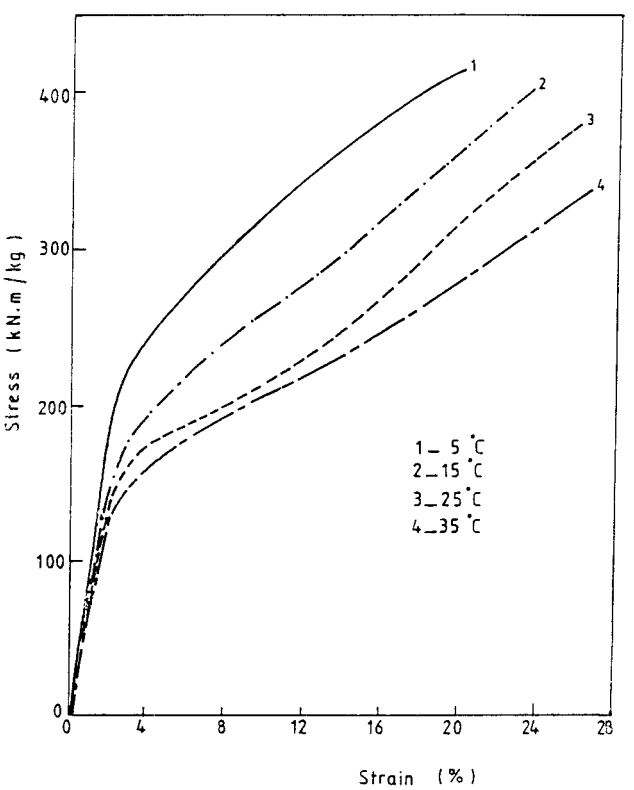

Figure 7 Stress–strain curves of FM fibers produced at different coagulation bath temperatures and drawn up to an 8.5 draw ratio.

The improvement in mechanical properties is well supported by the increased in sonic modulus. For instance, in FM the sonic modulus values increased from 13,388 to 13,805 kN m kg^{-1} for fibers drawn in the first (FM15) and second (FM15D) drawing zones.

Figure 9 shows the stress–strain curves of FA fibers collected at different stages. The effect of stretching and drawing was very much evident in that the drawing improved initial modulus and tenacity with a concomitant decrease in elongation at break.

Although the effect of coagulation bath temperature was more pronounced, the final fibers made from different copolymers did exhibit some interesting deviations among themselves. Figure 10 depicts the stress–strain behavior of three copolymer fibers coagulated at 5°C and drawn to a draw ratio of 8.5. Among these, acrylonitrile–methacrylic fibers exhibited higher modulus and tenacity compared to those of acrylonitrile–itaconic acid. Steric hindrance in the latter may be responsible for its relatively poor packing, leading to the higher extensibility and poorer tenacity of these fibers. In general, the X-ray orientation factor and sonic modulus of FI fibers is relatively low, which indicates lower orientation.

TABLE VII
Mechanical Properties of Fibers collected after Second Zone of Drawing (DR = 8.5)

Fiber code	Density (g/cm^{-3})	Tenacity [kN m kg^{-1} (cv %)]	Breaking elongation % (cv %)	Initial modulus [kN m kg^{-1} (cv %)]	Sonic modulus (kN m kg^{-1})
FA5D	1.182	413 (8)	22.5 (17)	8230 (11)	14,690
FM5D	1.180	428 (10)	20.6 (20)	8496 (12)	14,867
FI5D	1.178	387 (11)	23.1 (18)	7788 (8)	13,274
FA15D	1.180	368 (12)	25.8 (22)	7699 (10)	12,566
FM15D	1.176	400 (9)	23.3 (18)	7965 (13)	13,805
FI15D	1.180	358 (11)	24.8 (17)	7699 (11)	12,389
FA25D	1.175	357 (10)	27.8 (18)	7611 (12)	12,478
FM25D	1.174	377 (13)	25.7 (19)	7788 (12)	12,832
FI25D	1.172	321 (9)	29.2 (20)	7433 (10)	12,124
FA35D	1.172	326 (8)	31.7 (20)	7345 (13)	11,504
FM35D	1.169	338 (12)	26.6 (23)	7613 (14)	12,036
FI35D	1.168	303 (13)	33.8 (24)	7168 (13)	11,327

The crystallinity index of the FM fibers was also generally higher, with FA falling in between. The boiling water shrinkage of the fibers was reduced on further drawing because of improvement in the crystallinity. For instance, in FA25 this value was 10.1%, which reduced to 9.8% for the fiber drawn up to 8.5 DR (FA25D).

On drawing in the second drawing zone up to 8.5 DR, the moisture regain reduces. PI15 showed 1.7% moisture regain, whereas on further drawing (DR = 8,5) in PI 15D this value is reduced to 1.5%.

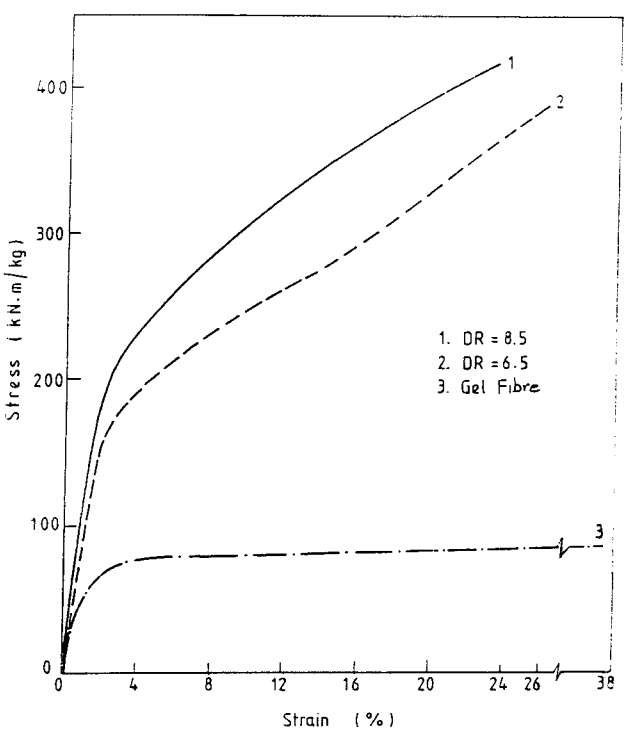

Figure 9 Stress–strain curves of acrylonitrile–acrylic acid copolymer fibers collected at different stages of spinning.

Thermomechanical studies

Thermomechanical shrinkage of these fibers heated at the rate of 10°C/min brought out interesting differences not previously observed in mechanical properties measured at room temperature. Figure 11 shows the TMA curves of these fibers.

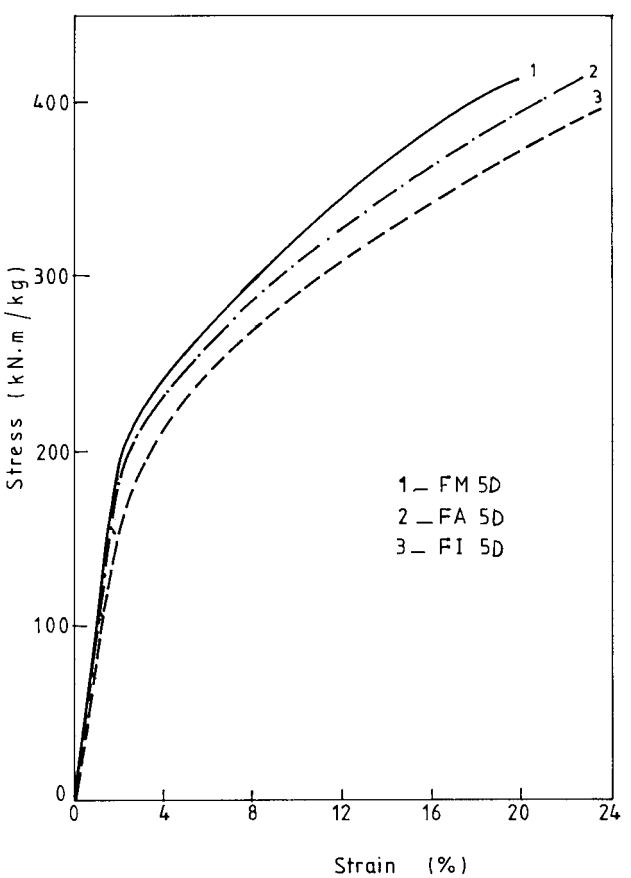

Figure 10 Stress–strain curves of acrylonitrile–carboxylic acid copolymer fibers FM5D, FA5D, and FI5D.

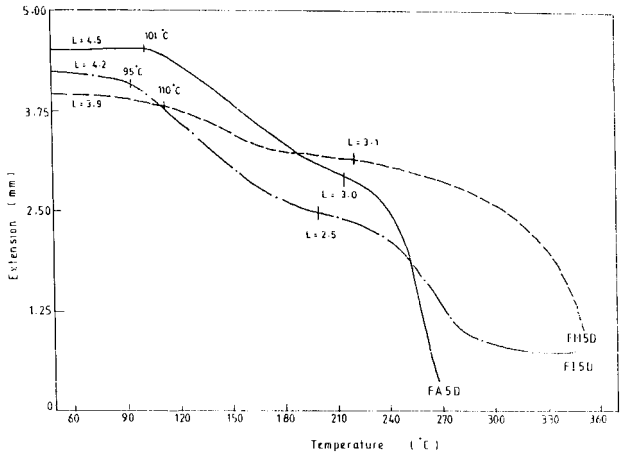

Figure 11 Thermomechanical curves of acrylonitrile–carboxylic acid copolymer fibers spun at 5°C coagulation bath and drawn up to an 8.5 draw ratio.

Thermal shrinkage in acrylic fibers is a two-step process. The first step could be attributed to the physical shrinkage that occurs because of the relaxation of the stresses that builds in the amorphous phase during fiber spinning and drawing; whereas the second step of thermal shrinkage could be a result of chemical reactions that lead to the cyclization of the nitrile group. The segmental mobility in the polymer chains starts as the temperature approaches the glass-transition temperature (T_g) and the process of physical shrinkage begins. The temperature of the onset of shrinkage was highest for FM5D, 110°C, and was lowest for FI5D, 95°C. This indicates the relative rigidity and better packing of the former, exhibiting high T_g of the AN–MAA copolymer. In addition, physical shrinkage was lowest in the FM5D fibers, indicating some of the entropic shrinkage had already occurred in the process of subsequent heat treatment (second-zone drawing). Shrinkage in the higher temperature range is related to chemical changes such as cyclization and dehydrogenation. These chemical changes started at a lower temperature for FI5D and FA5D fibers than for FM5D fibers. The influence of acidic comonomers, namely, AN, MAA and IA, in acrylonitrile copolymers was demonstrated using DSC–FTIR techniques.[41]

Fiber code	Thermal shrinkage %			
	Temp. range °C	Physical	Temp. range °C	Chemical
FA 5D	101–215	33.7	215–270	55.9
FM 5D	110–207	20.8	207–345	51.2
FI 5D	95–195	38.9	195–315	42.5

Physical shrinkage was lowest in FM5D, 20.8%, and highest in PI5D, 38.9%. The chemical shrinkage in PI5D began at a much lower temperature (195°C) compared to other fibers. This again demonstrates the effect of itaconic acid in initiating the cyclization reaction at a lower temperature.

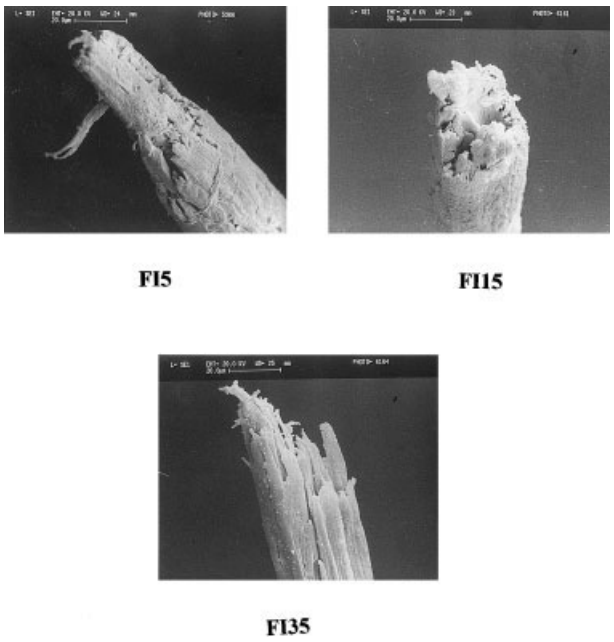

Figure 12 SEM fractographs of FI fibers spun at different coagulation bath temperatures and drawn up to a 6.5 draw ratio (first-zone drawing).

Fracture morphology

Fracture morphology has been related to the manufacturing processes of a number of acrylic fibers (341,

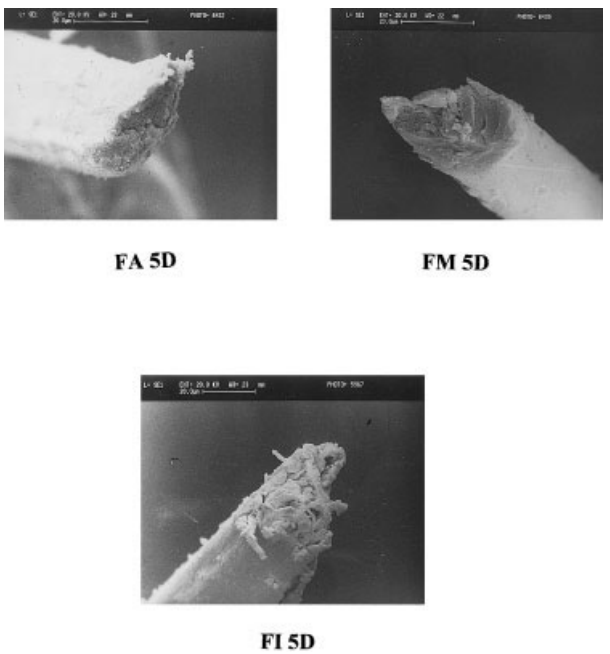

Figure 13 SEM fractographs of FI fibers spun from acrylonitrile–acrylic acid (FA5D), methacrylic acid (FM5D), and itaconic acid (FI5D) copolymers coagulated at 5°C and drawn up to a total draw ratio 8.5.

342). The effect of coagulation bath temperature and incorporation of different acidic comonomers on the fracture morphology of acrylic fibers is clearly evident in the scanning electron microscopy (SEM) fractographs shown in Figures 12 and 13.

As the coagulation bath temperature increased, the tensile fracture morphology changed. The acrylonitrile–itaconic acid copolymer fibers produced in the 5°C coagulation bath [DMF:H_2O 60:40 (v/v)] showed the fibrillar end of a long split break, indicating the tip and base of the split. The fracture seemed to have appeared from the sheath of the fiber, with core fibrillar ends elongated because of ductile failure [Fig. 12(a)], whereas the tensile fracture was nearly straight across the fiber, with little evidence of crack development near the voids present in the fiber cross section.

In FI35 the fracture was divided into widely separated fibrils joined by the split along the fiber axis. The matrix between the individual fibrillar fractures was probably drawn out and then fractured as the molecular chains were pulled straight. The separate bundles projecting from the main fracture surface [Fig. 5.13(c)] perhaps represent a situation in which rupture results from brittle failure.

The scanning electron micrographs of the tensile fracture morphology of the final fibers produced with a total draw ratio (TDR) of 8.5 are shown in Figure 5.14. Fracture occurred along the plane transverse to the draw direction with tapering showing in the cross sections of FA5D and FM5D. The tapering cross section was generally observed in fibers having high crystallinity. However, in FI5D the failure began from the skin, and the crack propagated through the matrix along the fiber axis. So, in PI5D and FM5D, it may have been ductile failure with parallel striations or grooves in the matrix of the latter.

The above investigation shows that coagulation bath temperature plays an important role in the physical and mechanical properties of spun fibers. The best mechanical properties were obtained from the fibers spun at the 5°C coagulation bath temperature. Among these, carboxylic acids fiber spun from copolymers of acrylonitrile–methacrylic acid showed better mechanical and physical properties. The additional drawing also improved the mechanical properties.

References

1. Sen, K.; Hajir Bahrami, S.; Bajaj, P. JMS Rev Macromol Chem Phys C 1996, 36(1), 1.
2. Poynton, D. J. Textile Prog 1976, 8(1), 51.
3. Burkinshaw, S. M. Chemical Principles of Synthetic Fiber Dying; Blackie Academic & Professional, Chapman & Hall: London, 1995.
4. Bajaj, P.; Pamanaban, M. Textile Res J 1985, 55, 352.
5. Frushou, B. G.; Knorr, R. S. In Handbook of Fiber Science and Technology; Lewin & Pearce, Eds.; Dekker: New York, 1985; Vol. IV.
6. Bajaj, P.; Sengupta, A. K.; Jain, P. C. Textile Res J 1980, 40, 218.
7. Mamazhanov, A. A.; Timoshina, L. V.; Zakirov, I. Z.; Ergashev, K. E.; Askarov, M. V. Khim Volokna 1990, 4, 22
8. Babenko, N.; Geller, A. A.; Geler, B. E.; Zakirov, I. Z.; Ubaidullaev, B. K.; Yakubova, N. Y. Khim Volokna 1972, 4, 66.
9. Yudin, A. V.; Shevehenko, A. S.; Pimoneko, E. P.; Bandura, N. A.; Kutin, V. A.; Vakovela, V. Y. Khim Volokna 1973, 5, 73.
10. Zakirov, I. Z.; Geller, B. E. Khim Volokna 1992, 4, 12.
11. Zakirov, Z.; Gellller, B. E. Khim Volokna 1993, 25(1),199.
12. Bajaj, P.; Kumari Munukutla, S. Text Res J 1990, 60, 133.
13. El Mogahzy, E. Y.; Broughton, R. M. Melliand Textilberichte 1995, 4 ,E52.
14. Qin, J. J Appl Polym Sci 1992, 44, 1095.
15. Stoyanov, A. I. J Appl Polym Sci 1982, 27, 235.
16. Suity, W. J Fiber Sci Tech, Jpn 1966, 22, 421.
17. Mejirov, M.; Jabin, V.; Pakshver, E. Collect Synth Fibres, Chemistry, Moscow 1969, 99.
18. Takahashi, M.; Watanabe, M. J Soc Text Cellulose Indr Jpn 1959, 34, 951.
19. Tsai, J. S.; Su, W. C. J Mater Sci Lett 1991, 10(1), 253.
20. Knudsen, J. P. Textile Res J 1963, 33, 13.
21. Han, C. D.; Segal, L. J Appl Polym Sci 1970, 14, 2973.
22. Takahashi, M.; Nukushina, Y.; Kosugi, S. Textile Res J 1964, 34(2), 87.
23. Takahashi, M.; Watanabe, M. Sen-i-Gakkaishi 1959, 15, 951.
24. Zwick, M. M.; Van Bochowe, C. Textile Res J 1964, 34, 417.
25. Takahashi, M.; Watanabe, M. Sen-i-Gakkaishi 1961, 17, 249.
26. Pakshever, E. A.; Barshokov, I. A.; Kireeva, N.; Kamskii, R. A.; Lobonova, G. A. Khim Volokna 1992, 1, 25.
27. Ergashev, E. A.; Zgbneva, S. A.; Slepakova, S. I.; Zhenqion, W. Adv Polym Technol 1968, 6, 509.
28. Terada, K. Sen-i-Gakkaishi, 1973, 29(8), T345.
29. Baojan, Q.; Jain, Q.; Zhenlong, Z. Textile Asia 1989, 48.
30. Badjun, G.; Ding, P.; Zhenquin, W. Adv Polym Technol 1986, 6, 509
31. Grobe, V.; Heyer, H. J Faserforsch Textiltech 1968, 19, 313.
32. Paul, D. R. J Appl Polym Sci 1968, 12, 383.
33. Rende, A. L. J Appl Polym Sci 1972, 16, 585.
34. Alieva, E. R.; Kozhernikov, Y. P.; Medvedev, V. A.; Serkov, A. T. Khim Volokna 1990, 5, 6.
35. Dolzhikov, V. B.; Zgibneva, Z. A.; Ergashev, K. E. Khim Volokna 1992, 2, 19.
36. East, G. C.; McIntayer, J. E.; Patel, G. C. J Text Inst 1984, 3, 196.
37. Gupta, B. C.; El-Mogahzy, Y. E.; Selivansky, D. J Appl Polym Sci 1989, 38, 899.
38. Rumyantseva, M. V.; Fomeko, B. A.; Pakshver, E. A.; Zhabin, V. D.; Tolkachev, Y. A. Khim Volokna 1992, 4, 41.
39. Law, S. J.; Mukhapadayay; S. K. J Appl Polym Sci 1996, 62, 33.
40. Law, S. J.; Mukhapadayay; S. K. J Appl Polym Sci 1997, 65, 2131.
41. Law, S. J.; Mukhapadayay; S. K. J Appl Polym Sci 1998, 69, 1459.
42. Law, S. J.; Mukhapadayay; S. K. J Text Inst 1998, 89(2), 182.
43. Law, S. J.; Mukhapadayay; S. K. J Text Inst 1999, 90(2), 137.
44. Bajaj, P.; Hajir Bahrami, S.; Sen, K. J Appl Polym Sci 1996, 59, 1539.
45. Tsai, J. S.; Lin, C. H. J Mater Sci Lett 1990, 9, 869.